Chapter 4 Experimental Studies

In Chapter 2, three improved order tracking techniques are theoretically developed. The fundamental ideas and logic of implementing these techniques are also described. In chapter 3, the abilities of these techniques are demonstrated in simple rotor and gear mesh simulation models. In this chapter, the techniques are demonstrated in real rotating machinery environments. Following the logic of the simulation studies, two experimental setups in the Sasol Laboratory for Structural Mechanics at the University of Pretoria are used to acquire rotating machine vibration signals. These setups comprise an automotive alternator set-up and a transmission gearbox test rig. Vibration signals are sampled in both good and seeded fault conditions. The first two techniques, VKC-OT and IVK-OT, are applied to signals from the alternator experimental set-up, in line with simulation studies in Chapter 3. And the gear box vibrations are used to illustrate the ability of the ICR technique.

4.1 Automotive alternator set-up data analysis

4.1.1 Experimental automotive alternator set-up

Wang and Heyns (2009) established an experimental set-up in Sasol laboratory for Structural Mechanics at the University of Pretoria, to investigate the ability of VKF-OT in condition monitoring. Typical run-up data (vibration and tachometer signals) from the automotive alternator were obtained. The experimental set-up is shown in Figure 4.1(a) and the monitoring process is schematically represented in Figure 4.2. The key components of the experimental set-up are the alternator, the variable speed motor, the controller and the battery. The alternator is driven

by a variable speed induction motor via a normal V-belt. The variable speed motor is controlled by a DC controller. The alternator charges an automotive battery which in this case is used as the system load.

a. Experimental set-up b. Monitoring devices

Figure 4.1 Experimental set-up

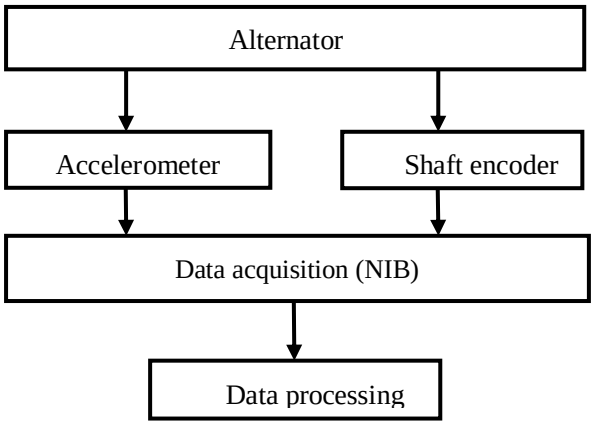

Figure 4.2 Monitoring process

The monitoring equipment for this experimental set-up, comprise an accelerometer and a shaft encoder, with a National Instruments Board (NIB) and computer. The accelerometer was mounted on the outer surface of the alternator (see Figure 4.1(b)), and the acquired signal was amplified and transferred through a PCB

amplifier and NIB to the computer. The rotational speed signal was monitored simultaneously through the shaft encoder, which was mounted on a specially made rotor shaft extender as is shown in Figure 4.3. The acquired signal first goes to the shaft encoder signal transfer box and then to the NIB before it finally also reaches the computer.

Figure 4.3 Shaft extender

4.1.2 Experimental fault description

An electrical short was artificially introduced on the stator windings. A blade was used to scratch off the resin on the outer isolation layer of windings at the location shown in Figure 4.4(b). This introduced an inter-turn short between the windings, referred to in this study as the seeded fault for the alternator experimental set-up. The original condition is shown in Figure 4.4(a). Since there are 36 winding bars, and an accelerometer which was mounted on the surface of the winding bars, this fault could be expected to influence orders which are multiples of 36. Thus for this alternator, the 36^{th} order or its multiples is of particular importance as a signature of the fault.

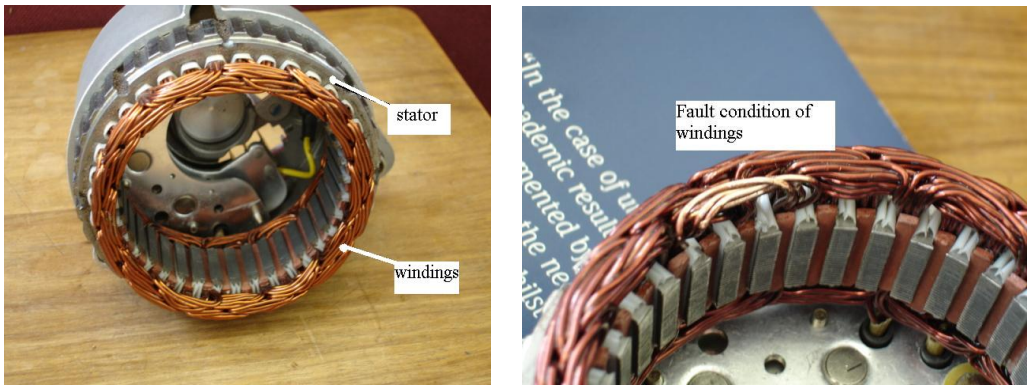

a. stator and windings b. seeded fault on windings

Figure 4.4 Seeded faults

4.1.3 Application of VKC-OT and IVK-OT techniques on the alternator experimental set-up

4.1.3.1 Application of Vold-Kalman filter and computed order tracking

This experimental set-up was first used by Wang (2008) to investigate the ability of VKF-OT in condition monitoring. Vibration signals obtained from this experimental set-up can also be used for verifying the ability of VKC-OT and IVK-OT. A typical set of measured data and the corresponding rotational speed is plotted in Figure 4.5, and shows how the vibration as well as the speed changes with time.

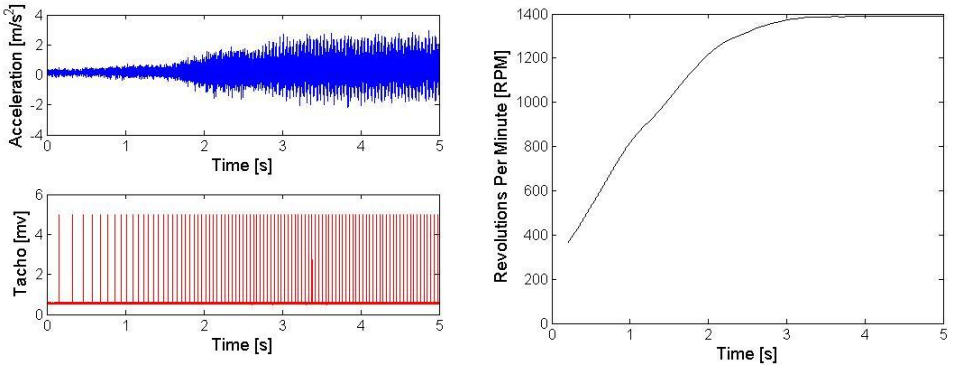

a. Measured data b. RPM

Figure 4.5 Raw data set

Clearly, this data is acquired during acceleration and the signal is quite non-stationary. Using this data, the VKC-OT technique can be applied here to extract a clear order component. Since there are 36 stator bars in the alternator, the Vold-Kalman filter is used here to extract the 36th order. Similar as to what have been done in chapter 3 of the simulation studies, some basic PSD analyses are performed. They are PSDs for the raw data, the 36th order by VKF-OT, computed order tracking and VKC-OT for the 36th order, and are plotted in Figure 4.6.

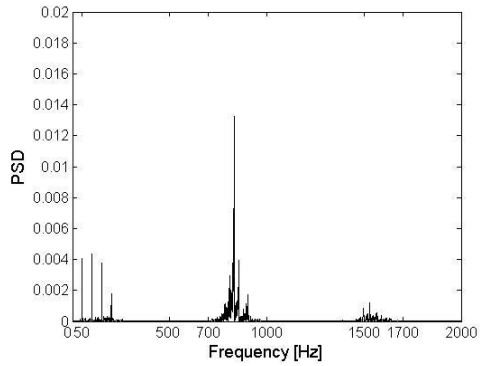

a. PSD on raw data

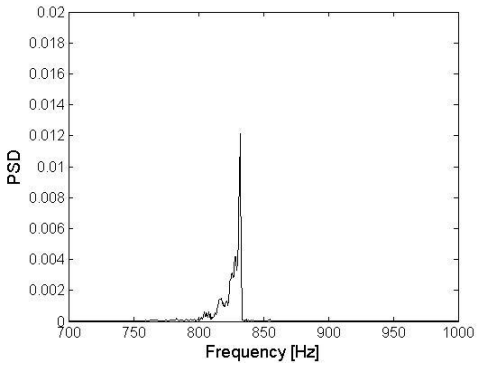

b. PSD on VKF-OT for 36th order

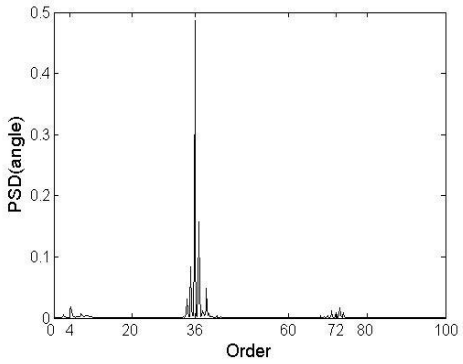

c. PSD on COT data

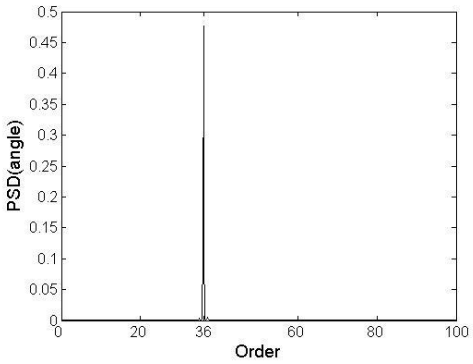

d. PSD on VKC-OT for 36th order

Figure 4.6 PSD results for alternator data

Figure 4.6(a) shows the PSD of the raw data. There are several frequency peaks around 50, 100, 150 Hz, and some higher frequency peaks around 700 – 1000 Hz and 1500 – 1700 Hz. Since the alternator output frequency is 50 Hz, it is expected to have frequencies at 50 Hz and its multiples. Besides, based upon the rotational speed measurement, full speed of the alternator can be seen to nearly approach 1400 RPM or ≈ 23.3 Hz. Since there are 36 stator bars, therefore $36 \times 23.3 = 838.8$ Hz and its multiples may appear, e.g. $72 \times 23.3 = 1677.6$ Hz. These two frequencies are clearly within these ranges of higher frequencies (700 – 1000 Hz and 1500 – 1700 Hz). It is however difficult to obtain any specific information from Figure 4.6(a).

If the Vold-Kalman filter based order tracking is performed with a relative filter bandwidth of 30%, the associated PSD spectrum is plotted in Figure 4.6(b) for the 36th order. In order to clearly see the filtered 36th order, the abscissa is zoomed over a range from 700 Hz to 1000 Hz. The 36th order is now much clearer than in Figure 4.6(a), but the smearing effect still exist and it is still not ideal for monitoring purposes. Figure 4.6(c) is the PSD (angle) of the COT result. It can be clearly seen that order 36 and its sideband orders are all included in the figure and also lower orders at around 4 as well as higher orders at around 72. It is however quite clear that it cannot focus on one order only and several order peaks are featured in the figure. The PSD (angle) does however not focus on one individual order component - in this case for example the 36th order which is of great importance for condition monitoring purposes. Finally, VKC-OT is applied to the data to extract the 36th order in Figure 4.6(d). It can be seen that a clear and clean 36th order peak exists which effectively excludes other sideband orders as well as the smearing effect. This result demonstrates the unique ability of VKC-OT technique which is intractable by using any of order tracking techniques in isolation alone. Therefore, by using VKC-OT technique, it achieves to represent a clear and individual order component in a real application.

4.1.3.2 Application of intrinsic mode function and Vold-Kalman filter order tracking

The proposed IVK-OT technique was subsequently applied to the same experimental set-up. Firstly, a data set corresponding to the alternator in good condition was considered. Again since there are 36 stator bars in the alternator, the 36th order and its multiples are key features of the signal. Therefore, EMD and VKF-OT were used to focus on the 36th order. The extracted 36th order by VKF-OT is used to compare the EMD results. In order to identify which IMF captured the 36th order, some basic frequency analysis was first performed.

Firstly, a frequency analysis of the Vold-Kalman filter result for the 36th order was done, and then a frequency analysis for each IMF was compared with the results from the Vold-Kalman filter. In this way, it was recognized that, in this case, the 6th IMF captured most of the energy associated with the 36th order. Figure 4.7 shows the results in the time domain as well as in the frequency domain.

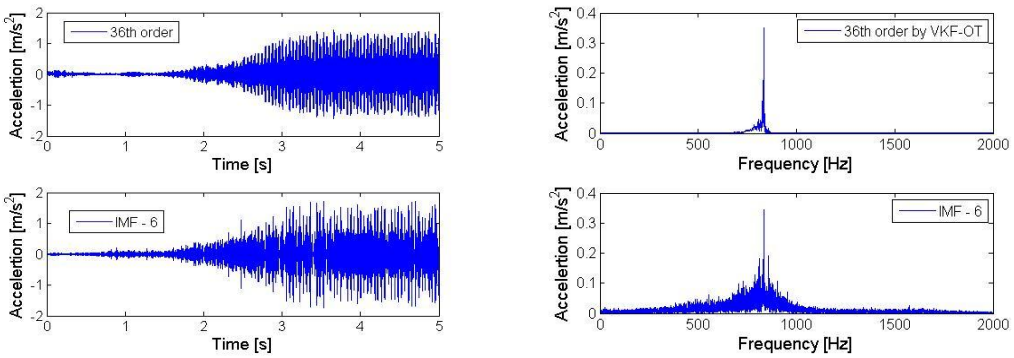

(a) Time domain waveforms (b) Frequency domain spectrum

Figure 4.7 The 36th order by VKF-OT and in IMF-6

It can be seen from Figure 4.7(a) that roughly speaking, the 36th order by VKF-OT and the 6th IMF are more or less equivalent in amplitude and shape. Strictly speaking, the result from VKF-OT is much cleaner and more uniform than its counterpart 6th IMF. This follows from the mathematical definition of equation (2.5) in which the sinusoidal nature is impressed on the filtered order of VKF-OT. Furthermore, the basic frequency analysis in Figure 4.7(b) shows that both the two time-domain waves capture the same fundamental frequency at around 838.8 Hz as has been calculated for the previous technique. However, it should be noted that the 6th IMF is obviously more complex than the 36th order by VKF-OT. This complexity is due to the resolution of the intrinsic mode function, in that all the signals that modulate the 36th order may be included, on condition that the final shape of the wave satisfies the requirements of an IMF. Clearly the 6th IMF captures the majority of the 36th order and the corresponding highest frequency

peak coincides with the Vold-Kalman filter result. The inclusion of other frequency components in one IMF is one of the shortcomings of EMD when extracting a mono-order component in real applications. However, it is also due precisely to this attribute that IMF may capture machine fault signals that modulate the order of interest. This observation from Figure 4.7 points to the possible further decomposition of the 36^{th} order related IMF and the decomposition of the signal may be useful for condition monitoring. Besides, it should also be borne in mind that the EMD process in fact separates the 36^{th} order together with vibrations that modulate it from other interference of orders, such as multiples of the 36^{th} order, like the 72^{nd} order. Therefore, all attention can now be focused on the modulated 36^{th} order.

From the experience gained in the simulation study in chapter 3, the computed order tracking results may help to recognize orders for signals. Therefore, in the following, COT is again used to transform all the analysis signals into the order domain. The 6^{th} IMF is then further decomposed. In Figure 4.8, the order domain results of the 6^{th} IMF, the Vold-Kalman filter for the 36^{th} order from 6^{th} IMF and the sequential use of the two techniques are presented.

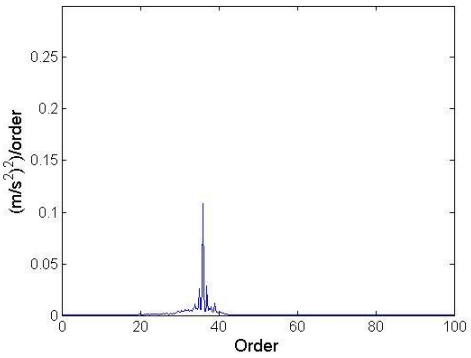

(a) 6th IMF

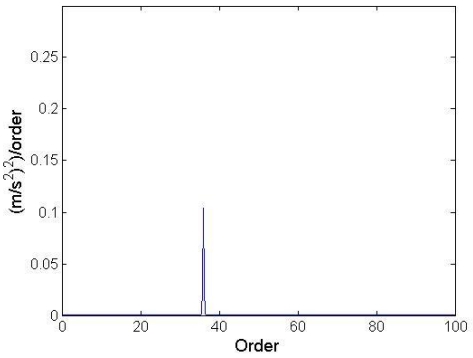

(b) Vold-Kalman filter order 36

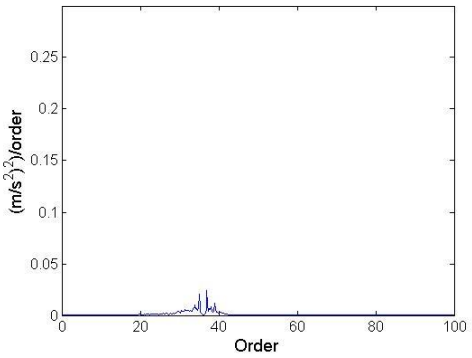

(c) Residue signal

Figure 4.8 PSD on 6th IMF, Vold-Kalman filter 36th order from 6th IMF and residue signal in order domain (good condition)

It is clear from Figure 4.8(a) that the 6th IMF includes the 36th order and some sidebands. After applying the Vold-Kalman filter, the 36th order is clearly extracted from the 6th IMF as shown in Figure 4.8(b). Figure 4.8(b) suggests that the Vold-Kalman filter succeeded in extracting the 36th order from the 6th IMF using a 20% relative filter bandwidth. Then the residue signal after sequential use of the two techniques contains the sidebands of the 36th order, as is depicted in the order domain as shown in Figure 4.8(c). Based upon the order domain analysis of the 6th IMF, it is clear that this IMF is dominated by 36th order signal. Only some sidebands are included. There are no other prominent orders appearing around the 36th order and therefore no need to further extract other

orders. Besides, as was learnt from the simulation studies, amplitude modulation may cause sidebands around dominant orders. This is a very useful indication of machine condition. Thus, the residue signals of the 6th IMF which hold sideband information will be useful for condition monitoring. This information cannot be extracted by traditional VKF-OT, but through further decomposition of 6th IMF. For illustration, the time domain residue signal is also plotted in Figure 4.9 (a) for this good condition data.

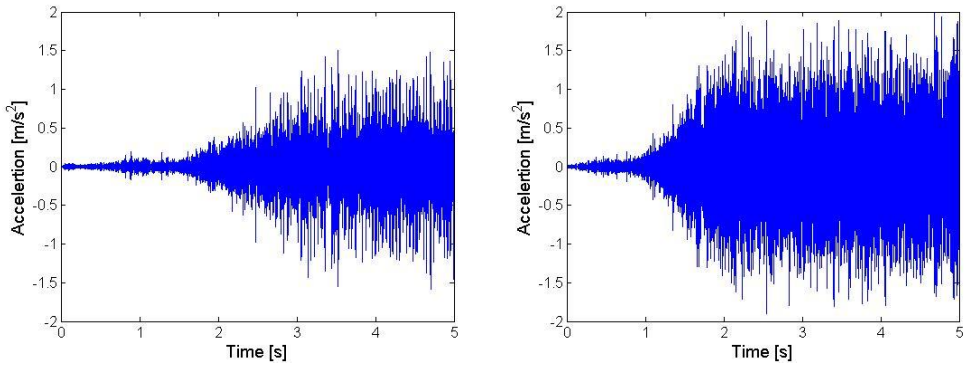

(a) Residue signal (good condition) (b) Residue signal (bad condition)

Figure 4.9 Residue signal in good and fault condition

The seeded fault signal is subsequently considered. The same COT analysis was again performed for 6th IMF, the 36th order by VKF-OT from 6th IMF and the results of combing the two techniques are shown in Figures 4.10(a), (b) and (c).

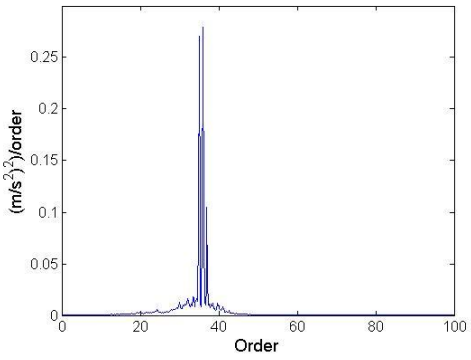

(a) 6th IMF

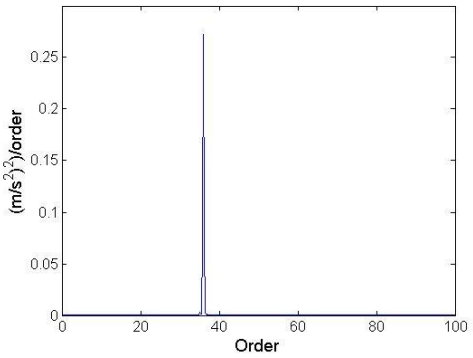

(b) Vold-Kalman filter order 36

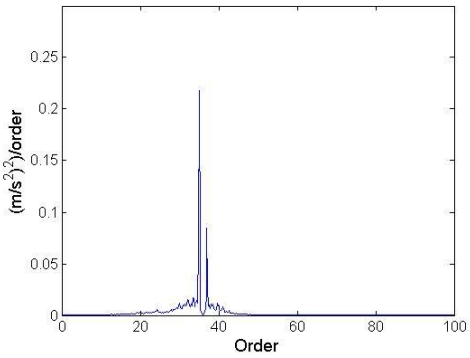

(c) Residue signal

Figure 4.10 PSD on 6th IMF, Vold-Kalman filter 36th order from 6th IMF and residue signal in order domain (seeded fault condition)

Due to the seeded fault, the amplitudes of the order component peaks in all three plots of Figure 4.10 have now clearly increased compared to the good condition shown in Figure 4.8. This is to be expected because the short circuit between the stator windings changes the electromagnetic field and causes changes in the vibration amplitude. This is especially the case for the 36th order, which corresponds to the 36 stator bars in the alternator. Clearly, Figure 4.10 again shows the successful decomposition of the 6th IMF. The corresponding time-domain residue signal is also plotted in Figure 4.9(b). When compared with its counterpart in Figure 4.9(a), the system changes can be clearly identified simply

from the amplitude of the two residue time-domain signals. Besides, the order domain peaks in Figures 4.10(b) and (c) have both substantially increased.

However, most importantly, with the help of order tracking techniques, 6th IMF has been further decomposed into 36th order and sideband residues. This kind of separated vibrations is not achievable by the EMD method or VKF-OT alone. Thus, the 36th order as well as its sideband information is available and it is worthwhile studying each part of the signal to track the system changes in this real case and see how the different parts of signals contribute to the overall changes. Therefore, one of the most frequently used time-domain techniques, namely root mean square (RMS) analysis, was used here to demonstrate the diagnostic ability of time-domain signals of different parts. Three RMS values were compared for good and seeded fault conditions, as shown in Table 4.1.

Table 4.1 RMS for different signals

Signals	RMS - good	RMS - seeded fault	$\frac{(RMS(fault) - RMS(good))}{RMS(good)}$
IMF-6	0.3244	0.5758	77.5%
36th order from IMF-6	0.1568	0.2686	71.3%
Residue	0.2770	0.4974	79.57%

It can be concluded from this table that the changes in the 6th IMF are caused by both the 36th order and its residue. Clearly the RMS values of all of these signals change substantially. This result is reasonable, since the seeded fault in the inter-turn short circuit in the stator winding would influence the vibrations of both the 36th order and its sidebands. An inter-turn short in the stator windings of an alternator would not introduce simple parameter changes in the system but

influences the electromagnetic forces between stator and rotor in that entire area so that the vibration amplitude in that area is disturbed. Consequently, it should be expected that both order signals and sideband signals would be influenced by the introduction of the seeded fault. However, the further decomposition of the 6th IMF enables detailed studies of 36th order and its sideband vibrations in the time domain. For this specific case, changes in the sidebands to the residue signal are higher than the changes in the 36th order, by 79.57% and 71.3% respectively. Both of these signals are indicators of the stator inter-turn short. However, different part of signals may indicate the changes of different scenarios of machine conditions. When both the 36th order and its sidebands increase evenly, it means the whole electromagnetic force is increased, whereas, if additional sidebands increase compared to the dominant 36th order, this means that more amplitude modulation occurs.

Thus, from these detailed studies of the signals, it may be deduced that, after introduction of the seeded fault, the amplitude modulations of the 36th order become more severe than for the good condition. This is a clear indication of a machine inter-turn short which causes the change of electromagnetic force in a certain area and result in amplitude modulation of vibrations in the 36th order. As a result, the further decomposition of 6th IMF in this experimental study provides a method to examine in detail each part of the signal so as to provide in-depth understanding of machine condition. The experimental study therefore demonstrates that IVK-OT technique may be employed to further decompose the IMFs and therefore provides additional diagnostic capabilities for distinguishing and evaluating fault severity in machine vibration signals.

4.2 Transmission gearbox set-up data analysis

4.2.1 Experimental gear box set-up

For illustration of the ICR technique in condition monitoring, the technique is now demonstrated in a real working environment on signals from an experimental gearbox. The gearbox test rig was designed to conduct accelerated gear life tests on a Flender E20A gearbox under varying load conditions at the University of Pretoria Sasol Laboratory for Structural Mechanics. The experimental set-up consisted of three Flender Himmel Motox helical gearboxes, driven by a 5 kW three phase four pole Weg squirrel cage electrical motor. A 5.5 kVA Mecc alte spa three phase alternator was used for applying the load. The direct current (DC) fields of the alternator were powered by an external DC supply in order to control the load that was applied to the gears. A sinusoidal load with minimum to maximum loads from 7.4 to 14.7 (Nm) was applied to the alternator. Two additional Flender E60A gearboxes were incorporated into the design in order to increase the torque applied to the small Flender E20A gearbox which was being monitored shown in Figure 4.11. The gear mesh frequency is 215Hz at 5 Hz shaft rotational speed. For details about the test rig the reader may also refer to the paper by Stander and Heyns (2006) and the master's dissertation of Schön (2006). In this case however the response measurements were taken with a Polytec PDV-100 laser Doppler vibrometer with a 500 mm/s measurement range (see Figure 4.11).

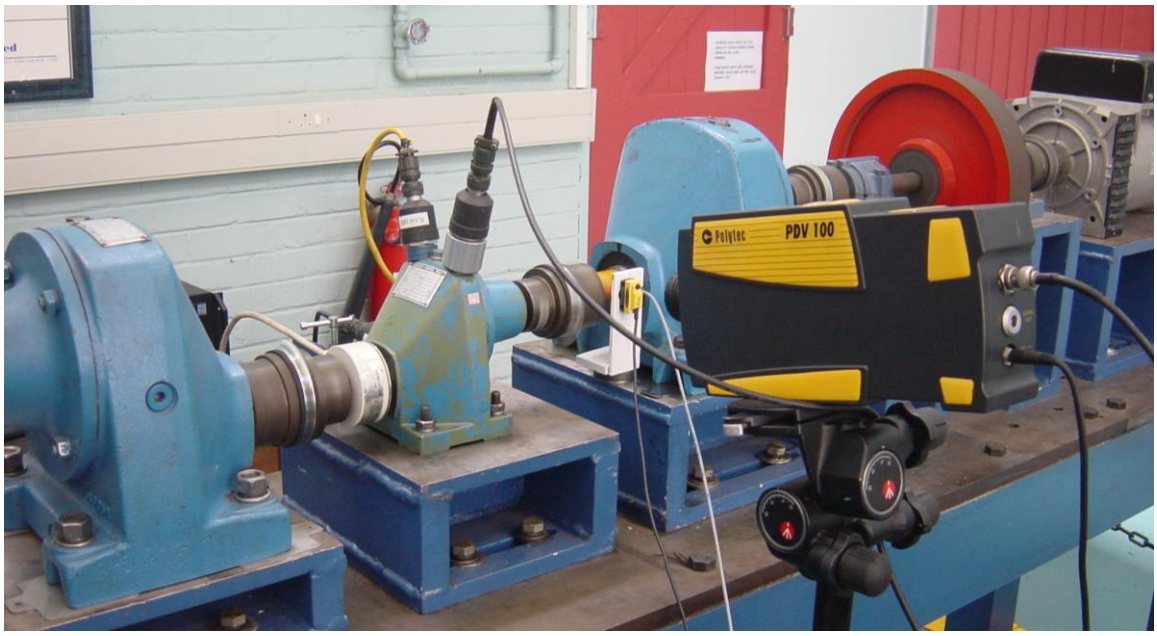

Figure 4.11 Experimental test rig

4.2.2 Experimental fault description

During the experimental process, the gear in Flender E20A gearbox at the centre of the set-up, was artificially damaged through overloading. This resulted in severe wear which eventually culminated in several broken teeth and ultimately stripped gear teeth. The original shape of the drive gear and its final state when all the teeth are removed are shown in Figure 4.12(a) and (b). However not all the obtained data is being considered in this experimental study. Only the data when the first gear tooth is removed is being used for the seeded fault studies in this experimental set-up.

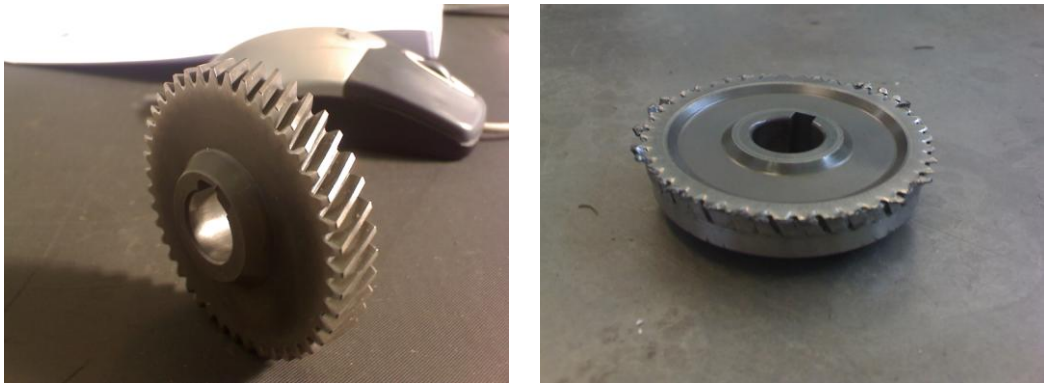

a) Original status of drive gear b) Final status of drive gear

Figure 4.12 Gear damage

4.2.3 Application of intrinsic cycle re-sampling

a. Traditional signal processing analysis on good condition

The monitored gearbox was set to run at about 300 rpm. To begin with, a 2 s signal was measured before damage was first introduced. The time domain waveform with the corresponding rotational speed, frequency spectrum of the translational velocity and computed order maps around 1× gear mesh order are shown in Figure 4.13.

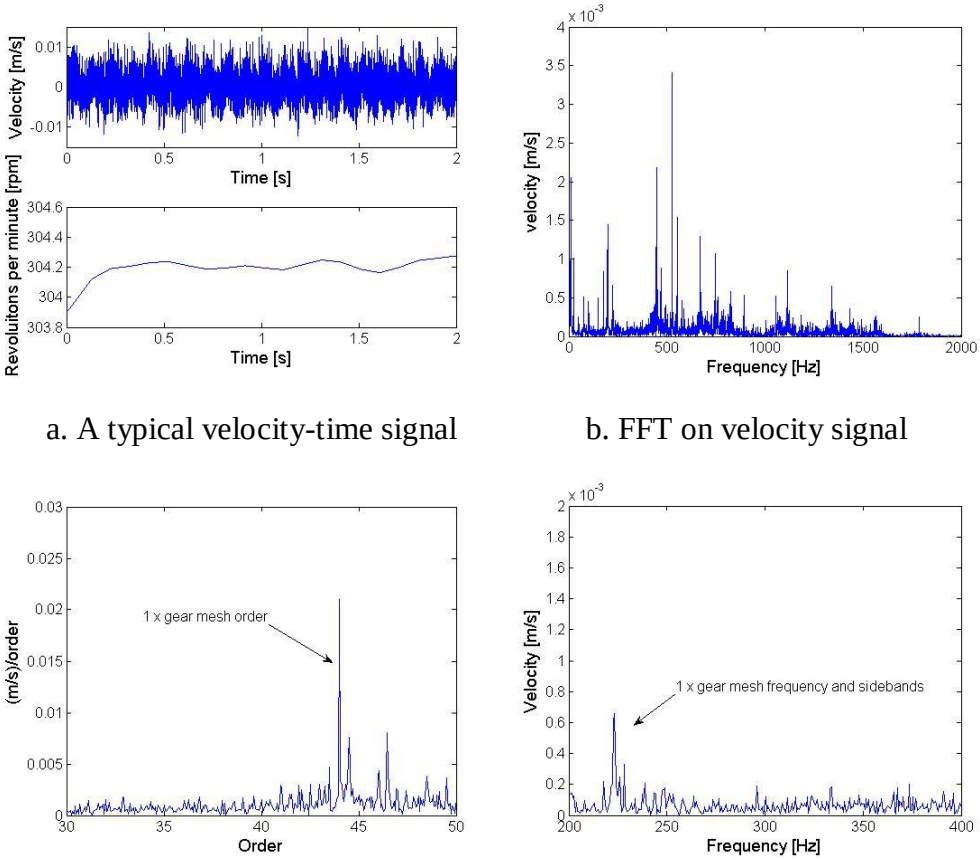

a. A typical velocity-time signal b. FFT on velocity signal

c. Computed order tracking d. Zoom in for 1× gear meshing frequency

Figure 4.13 Traditional signal processing methods

In these figures no damage has been introduced yet and no clear impacts occur in the time domain signal (Figure 4.13(a)). However amplitude modulation is visible throughout the period. Although the gearbox operates in a stable condition, the load fluctuation influences the rotational speed which leads to the frequency variation in the signal. From the Fourier analysis (Figure 4.13(b)) it is clear that the real gearbox data is much more complex than the simulated signal in chapter 3. Many frequency peaks appear throughout the spectrum. For condition monitoring purposes, we focus on the gear mesh frequency in the frequency spectrum. The spectrum after zooming in around 1× gear mesh frequency is shown in Figure 4.13(d). In figure (d), some sidebands around the

gear meshing frequency are also visible which are spaced at approximately 5 Hz. This corresponds to the rotational frequency of the gear. As expected the sidebands for the undamaged gear are few and small. The computed order tracking map in Figure 4.13(c) which zooms in around $1\times$ gear mesh order is also plotted. It should also be noted that although the order analysis excludes the speed variation effects, the spectra are still fairly complex and show several order sidebands around the gear mesh order.

b. Choosing an appropriate IMF

Once one has a basic understanding of the raw signal, EMD may be applied to the signal to extract the gear mesh information for further ICR application. The 5th to 8th IMFs are plotted in Figure 4.14 as velocity as a function of frequency.

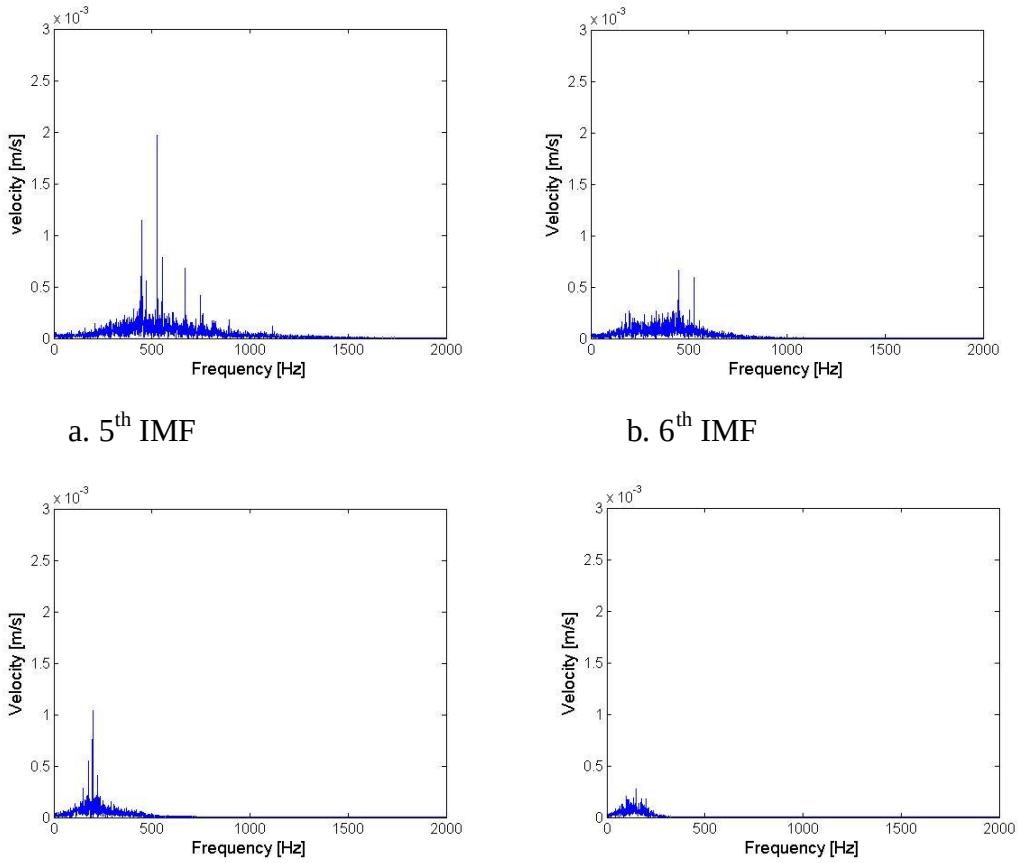

a. 5th IMF b. 6th IMF

c. 7th IMF d. 8th IMF

Figure 4.14 IMFs of system response

It can be seen from Figure 4.14 that the 7th IMF captures the signal content which is relevant to the nominal gear mesh frequency at 215 Hz. Although some energy is present in the 6th and 8th IMF, this is however fairly small. For the 5th IMF very little energy is observed in that range. As a result, the 7th IMF is of great importance for condition monitoring of gear mesh conditions. Therefore ICR is performed on the 7th IMF and result is shown in Figure 4.15. The result shows that the sidebands around the main frequency peak are oscillating and a clear two distinct sidebands appear around main frequency peak. The whole spectrum only concentrates on frequency range from 150 Hz to 250 Hz in which only those gear mesh related vibrations are being focused. Outside this frequency range, spectrum becomes negligible. This is very different from traditional methods as in Figure 4.13. In this case, the main frequency component is located at 210 Hz which is very close to the calculated nominal gear mesh frequency at 215 Hz, it is clear that the 7th IMF captures the gear mesh vibrations for this good condition case data.

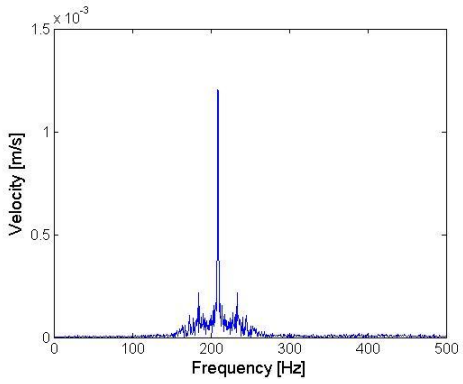

Figure 4.15 ICR on 7th IMF result

c. Traditional signal processing methods on fault detection

Once the seeded fault as described in the experimental set-up has been induced, the measured signals were considered over the same period as before. Firstly,

traditional signal processing methods are used to detect the system changes. Thus, time, frequency and order domain results are analyzed and compared in different figures as is shown in Figure 4.16. In order to clarify the differences between figures, the results for good and seeded fault conditions are superimposed on the same plot and normalized in terms of the highest frequency or order peaks that in frequency and order domain.

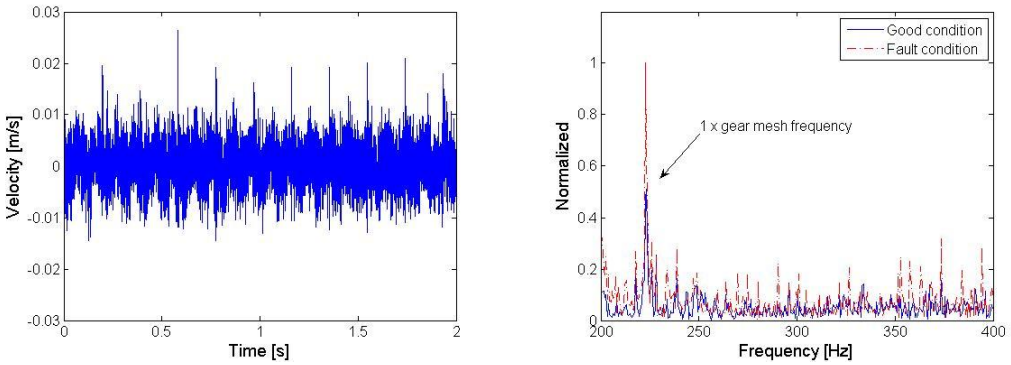

a. Time domain signals (fault) b. Zoomed in 1 × gear meshing frequency

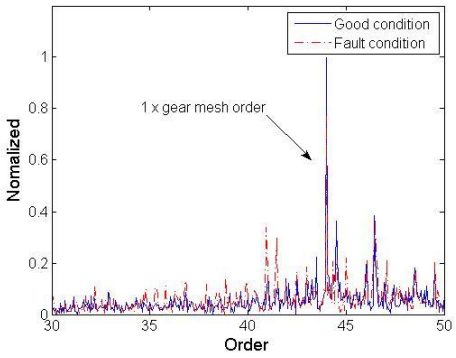

c. Zoomed in 1 × gear mesh order

Figure 4.16 Signals with broken tooth

Firstly, Figure 4.16(a) clearly shows that a periodic impact occurs in the signal, and that the period of this impact is approximately 0.2 s with a corresponding frequency of 5 Hz, which suggests that this impact occurs once per revolution. This is consistent with the induced fault scenario. Secondly, in the frequency

domain, it shows that more sharp sidebands appear in the spectrum and all the amplitudes of frequency peaks are increased, especially the 1× gear mesh frequency component. It is well known that if additional sidebands appear and existing sidebands increase around the gear mesh frequency, this indicates a broken gear tooth problem in the gearbox. Further, computed order analysis comparisons in Figure 4.16(c) again confirms that extra orders around gear mesh order increased due to the seeded fault on gear teeth, but it also shows that relative amplitude of several order sidebands compared with gear mesh order does not change as much as happened in the frequency domain. However, in this case, the additional order sidebands show the detection of the changes for gear mesh conditions. In short, experimental studies using traditional time, frequency and order domain methods achieve the detection of the seeded fault.

d. ICR result on seeded fault gearbox data

ICR is then applied to the faulted gear experimental data. In order to clearly show the difference of the spectrum before and after the seeded fault, the figure is also superimposed with the good condition result and normalized in terms of highest peak. Figure 4.17 shows the results.

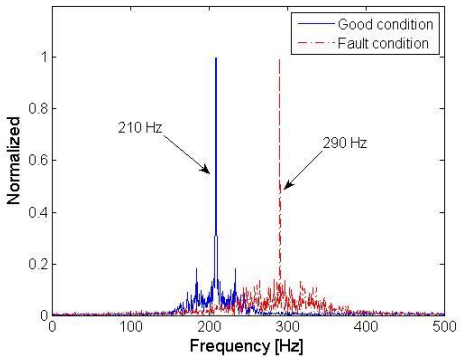

Figure 4.17 ICR result on faulted gear experimental data

As was learnt from the simulation studies in chapter 3, two aspects of the ICR results which respond to faults, are examined in Figure 4.17. These are M.F. and S.V. Clearly, for the seeded fault case, the M.F. value displays a significant shift from 210 Hz in good condition to 290 Hz. This is a clear indication of the increase of ICs, therefore a shift of f_{ICR}. From the perspective of S.V., firstly, the sidebands changed dramatically, therefore, the variation of the signal could not merely have been caused by rotational speed. This corresponds to chapter 2 paragraph 2.3.2 guideline (b). Secondly, although the highest sideband amplitudes do not change dramatically relative to the main frequency peak in the fault condition, many more sideband peaks appear in the spectrum. This is very different from the good condition where two highest sidebands appear distinctly. This indicates that the amplitude modulation part $A_{ICR}(t)$ of the seeded fault case is fundamentally changed. The above observations correspond to chapter 2 paragraph 2.3.2 guidelines (c) and (d). Clearly the fault introduced here does not represent a trivial influence to the gear mesh vibrations, which is consistent with the known broken gear tooth damage.

In short, observations from the ICR results clearly show the changes in the gear mesh vibrations. Comparing Figure 4.16(b), (c) and Figure 4.17 in frequency, order and ICR results respectively, it is not difficult to determine that the ICR technique provides simple and clear indicators for detecting the changes in terms of M.F. and S.V., especially for the distinct shift of M.F. However traditional methods will present many sidebands and amplitude variations in frequency or order domain which may complicate the process of decision making on fault diagnostic. As a result, compared with traditional methods in fault diagnostic in this experimental study, ICR provides effective and unique indicators for detecting seeded fault which make ICR technique can be a good alternative method to condition monitoring.

4.3 Summary

The two experimental setups provide opportunities to verify the three improved order tracking techniques in real rotating machinery environments. The VKC-OT technique presents its unique ability of featuring an individual clear order component under the varying rotational speed. The IVK-OT technique separates the order component and those vibrations that modulate order in an IMF which provides a deep understanding and ability to track machine conditions. The ICR technique transforms complicated gear mesh vibration related IMFs into simple signal spectrum figures which first empirically exclude frequency variation effects in the signal and then features more specific indicators, namely sidebands variations (S.V.) and main frequency component (M.F.), for condition monitoring. The experimental studies confirm the abilities of all three improved order tracking techniques.

Chapter 5 Conclusions

5.1 Contributions of the research

5.1.1 A brief review of the development of three improved order tracking approaches

As have been reviewed in chapter 1, various kinds of order tracking methods are presented in the literature. In this research, however three widely available and proven effective order tracking methods were chosen and studied to explore their characteristics in relation to each other, so that improved order tracking approaches could be developed for the purpose of condition monitoring rotating machines. The three methods that have been selected for developing the improved approaches are computed order tracking (COT), Vold-Kalman filter order tracking (VKF-OT) and the extraction of intrinsic mode functions (IMFs) through empirical mode decomposition (EMD).

Each of the techniques has their own advantages and disadvantages in different applications. Through the discussions of these pros and cons in chapter 1 paragraph 1.2, improved approaches to order tracking by combining these methods are presented in Table 1.1 and explained thereafter in chapter 1. This leads to the further development of advantages and avoidance of limitations to order tracking analysis by combing these three order tracking methods, namely (as is indicated in Table 1.1) VKF/COT, IMF/VKF and IMF/COT. Further, in the scope of work as outlined in paragraph 1.4 (Figure 1.4), the inter-relationships between the different order tracking methods are schematically depicted. Three improved order tracking approaches are formally introduced, namely Vold-Kalman filter and

computed order tracking (VKC-OT), Intrinsic mode function and Vold-Kalman filter order tracking (IVK-OT) and Intrinsic cycle re-sampling (ICR).

These three improved approaches may be summarised as follows:

VKF/COT →VKC-OT:

COT and VKF-OT are complementary to each other with respect to specific advantages and disadvantages. On the one hand, COT transforms non-stationary time domain data into the stationary order domain, while VKF-OT does nothing to transform the data to stationarity. On the other hand, COT cannot focus on each individual order as can be done by VKF-OT. Therefore, the combined application of the two methods is developed, namely VKC-OT.

IMF/VKF →IVK-OT:

VKF-OT results can constitute components of IMFs. Firstly, VKF-OT exhibits excellent filtering abilities for the extraction of order components. However precisely because of this ability to focus on orders of interest, it is incapable to capture the vibrations that modulate the orders, especially for speed non-synchronous vibrations. IMFs from EMD, however include both order vibrations and vibrations that modulate orders. Therefore, VKF-OT is used to further decompose the IMFs so that the orders as well as the vibrations that modulate them, can be separated for condition monitoring purposes. As a result, the IVK-OT method is developed.

IMF/COT→ICR:

IMF and COT in fact are not directly related. However, the advantages of the especially simple data structure of an IMF and the idea of re-sampling to transform

non-stationary data to stationary data in COT can be reconciled so that the ICR technique may be developed, and approximated order tracking effects on the IMFs can be achieved. This offers benefits for condition monitoring.

Through the development of the approaches in chapter 2 and the simulation and experimental demonstrations in chapters 3 and 4, the nature of the improved order tracking approaches become clear and are proven effective.

In the following the improvements offered by the proposed approaches are elaborated upon. These approaches are subsequently discussed in the context of condition monitoring.

5.1.2 Contributions of each improved order tracking approach

Vold-Kalman filtering and computed order tracking (VKC –OT)

This specific technique is mainly for extracting order components and excluding speed variation effects to render simple order components in the order spectrum. Advantage is taken from the definition of Vold-Kalman filter order tracking to extract and ensure the harmonic nature of an order component. In addition advantage is also taken from the re-sampling ability of computed order tracking to transform non-stationary effects due to the variation of rotational speed into stationarity. The contributions of this technique are primarily:

1. The analyst may focus on orders of interest which may be non-dominant amongst the signals and signals are strongly influenced by rotational speed.

2. Due to the use of VKF-OT, the VKC-OT technique has been imparted with the ability of extracting harmonic and smooth order signals and at the same time COT transforms non-stationary data to stationary data due to the variations of

rotational speed. Thus, the signals after application of VKF-OT and COT become more suitable for subsequent Fourier analysis and therefore render clearer order spectra for condition monitoring purposes.

In short, the VKC-OT technique capitalise on the advantages of VKF-OT and COT to present focused and clear order spectra. Again, the advantages of VKF-OT in terms of its strict mathematical filter to focus on orders of interest, and COT in its re-sampling procedure to exclude speed variation effects in signals, make the VKC-OT method more focused on orders of interest than COT and results in cleaner spectrum results than VKF-OT.

Intrinsic mode function and Vold-Kalman filter order tracking (IVK-OT)

This technique is specially developed for further decomposition of IMFs from EMD. The EMD process may decompose signals into different IMFs ranging from high to low frequency content. Applying this process to rotating machine vibration signals may separate order signals into different IMFs. These order related IMFs differ from traditional order tracking results such as VKF-OT. For one order related IMF, order signals together with vibrations that modulate orders are all possible to be included in an IMF. And these vibrations that modulate orders may consist of speed synchronous and non-synchronous vibrations. However traditional order tracking methods, e.g. VKF-OT, can only focus on vibrations that are synchronous with rotational speed. In reality, rotating machinery fault vibration signals are very likely in the form of vibrations that modulate order signals. These vibrations that modulate orders may therefore contain abundant machine condition information and not necessarily all synchronous with rotational speed. The IVK-OT technique is thus used to further decompose order related IMFs in terms of rotational speed, so that speed synchronous order vibrations and other vibrations that modulate orders in IMFs may be further distinguished. An important area - speed non-synchronous vibrations that modulate orders - that

un-extractable through EMD and traditional order tracking methods can be approached through IVK-OT technique. In summary, contributions of this technique lie in:

1. By using EMD the analysis exploits its powerful empirical nature which allows obtaining results which are intractable by most order tracking techniques. This empirical decomposition process can separate vibration orders into different IMFs. Each IMF is very similar to order tracking results, such as VKF-OT.

2. The relationship between an order and an IMF is discussed in this research and it is clear that this issue has not been properly discussed by researchers in the current literature. Thus another contribution of this work is the introduction and discussion of this issue.

3. Vibrations that modulate order components in the time domain (especially those vibrations that are non-synchronous with rotational speed) is captured. This is intractable by using other order tracking techniques and useful for rotating machinery fault diagnosis.

4. The adaptive nature of both IMF and VKF-OT allows the IVK-OT technique to follow the changes of non-stationary signals due to variations of rotational speed. Both of the techniques can also be treated as filters, therefore the IVK-OT technique is a kind of adaptive filter method to deal with non-stationary rotating machine vibrations.

In conclusion, from the theoretical point of view, the discussion on technique provides a description of the relationship between an order and an IMF which fills a gap in the literature. From the condition monitoring rotating machinery point of view, the IVK-OT technique provides an adaptive and order focused method to diagnose rotating machines and further provides the ability to separate vibrations

that modulate orders, especially those vibrations that are not synchronous with rotational speed. The vibrations that modulate orders are often useful indicators of machine faults and may not be easily extracted by EMD or traditional order tracking methods in isolation alone.

Intrinsic cycle re-sampling (ICR)

The ICR technique is based upon IMF from EMD. Taking advantage of the simple data structure of IMF, the novel concept of an intrinsic cycle (IC) is introduced. Further, considering computed order tracking technique in dealing with non-stationary rotational speed vibrations, the re-sampling idea is borrowed into an IMF through ICs so that the frequency variation effects due to rotational speed can be largely excluded between ICs in an IMF. The contributions of this technique are:

1. The result of this technique offers a simple method to approximate computed order tracking effects without the need for a rotational speed measurement, which makes this a practical albeit approximate approach for real vibration monitoring.

2. Through the exclusion of speed variation effects by empirical re-sampling ICs on an IMF, ICR provides unique frequency domain indicators for condition monitoring. The exclusion of frequency variation effects makes the interpretation of a re-sampled IMF more specific than the original IMF. It provides a simple and alternative method for the analyst to understand the condition of machines.

In short, the novel idea of using ICs in IMF and the borrowed idea of signal re-sampling from COT enables ICR to empirically exclude non-stationary rotational speed influences and approximate computed order tracking effects, so that the

re-sampled IMF becomes more specific to interpret and is therefore beneficial for condition monitoring on rotating machinery. The ICR technique as a possible alternative vibration monitoring tool and was demonstrated to render useful results.

5.1.3 Contributions of the three improved order tracking approaches as a whole in order related vibration signals

The previous discussions emphasised the usefulness of all three improved order tracking approaches in their own right. However, their contributions as a whole essentially provide a useful platform for order tracking analysis in condition monitoring. In the context of condition monitoring of rotating machines, order tracking analysis basically need to address two classes of vibration signals. Traditionally, order tracking analysis only focuses on the speed synchronous vibrations. But, vibrations that modulate order signals are also very important information for condition monitoring. Therefore, this is an indispensable part of order tracking analysis in terms of condition monitoring. The three improved order tracking approaches are in fact developed for dealing with both of these classes of vibration. Table 5.1 summarises the emphasis of the three improved order tracking approaches.

Table 5.1 Emphasis of three improved order tracking approaches

	0rder vibrations	Vibrations that modulate orders
VKC-OT	√	
IVK-OT		√
ICR	√	√

Firstly, the VKC-OT method is developed to focus on obtaining better order spectra of speed synchronous orders. Only speed synchronous order signals are

considered in this technique. Therefore, the technique is useful for order vibrations. Secondly, the IVK-OT method is developed to separate vibrations that modulate orders through which IMFs can be further decomposed in terms of rotational speed (see Table 5.1). The vibrations that modulate orders, therefore, can be achieved. Lastly, both order signals and vibrations that modulate orders are considered as a whole in the ICR technique. Signal changes in order related vibrations as well as in vibrations that modulate orders, will all be reflected in re-sampled IMF through ICR. As a result, the ICR technique addresses both order vibrations and vibrations that modulate orders, as is indicated in Table 5.1. In short, three improved order tracking approaches have been developed for contributing to order tracking analysis of rotating machinery condition monitoring. Each of these techniques is complementary in the overall perspective of order tracking analysis.

5.2 Future work

In this work, efforts have been focussed on developing improved order tracking techniques. Further applications of these techniques in real practice are needed. Systematically integrating three improved order tracking approaches into current condition monitoring software packages is also useful for enhancing abilities of order tracking analysis.